and it is, therefore, unlikely that after detachment of the first H atom, a second H atom would be eliminated. Little can be said concerning the modes of formation of the pentenes, except that they are related to those of hydrogen.

ACKNOWLEDGMENT

The authors would like to express their gratitude to the referee of this paper for his comprehensive comments on the discussion.

THE JOURNAL OF CHEMICAL PHYSICS VOLUME 47, NUMBER 12 15 DECEMBER 1967

Investigation of Some Ce^{3+}-Activated Phosphors

G. Blasse and A. Bril

Philips Research Laboratories, N. V. Philips' Gloeilampenfabrieken, Eindhoven, Netherlands

(Received 14 August 1967)

The fluorescence of a number of new Ce^{3+}-activated phosphors is described and discussed. Only host lattices with a sublattice consisting of trivalent lanthanide ions are used to avoid charge compensation of the Ce^{3+} ion. Usually the Ce^{3+} emission is in the near-ultraviolet region. $Y_3Al_5O_{12}$–Ce and SrY_2O_4–Ce, however, show emission in the visible region with a maximum in the green. Conditions for visible Ce^{3+} emission are indicated, viz., large crystal-field splittings ($Y_3Al_5O_{12}$–Ce) or a large Stokes shift (SrY_2O_4–Ce). In a number of cases we were able to observe all crystal-field components of the excited $5d$ level of Ce^{3+}. The cubic crystal-field splitting of the $5d$ level varies strongly with host lattice from 7000 to 14 000 cm^{-1}. The position of the center of the $5d$ levels in oxides is about 30% lower than in the free ion. For some phosphors we observed more than one emission band at room temperature. This is due to fluorescence from higher excited levels. Efficient energy transfer from Ce^{3+} to Cr^{3+} was observed in $Y_3Al_5O_{12}$.

I. INTRODUCTION

The fluorescence of Ce^{3+}-activated compounds is well known.[1,2] Usually the emission consists of a broad band with two peaks in the long-wavelength ultraviolet region. Since the Ce^{3+} ion has a $4f^1$ configuration, the ground state consists of a doublet ($^2F_{5/2}$ and $^2F_{7/2}$). The lower excited states are the crystal-field components of the $5d$ configuration. The transition $4f \rightarrow 6s$ and charge-transfer transitions are at considerably higher energies[3] and are not considered in this paper. The Ce^{3+} emission is due to a $5d \rightarrow 4f$ transition. This is an allowed electric dipole transition and therefore the decay time of the fluorescence is very short ($<10^{-7}$ sec).[1,4]

Recently we have also reported on a Ce^{3+}–phosphor which emits in the visible, viz., $Y_3Al_5O_{12}$–Ce.[4] This peculiar behavior prompted us to study the Ce^{3+} fluorescence in other oxides of the trivalent lanthanides (La^{3+}, Gd^{3+}, Y^{3+}, Sc^{3+}). Surprisingly enough, these materials have not widely been investigated, although these host lattices offer the possibility of introducing Ce^{3+} without charge compensation.

The present paper gives the results of this investigation. The complete crystal-field splitting of the $5d$ configuration of the Ce^{3+} ion was found in a number of cases. Requirements for Ce^{3+} emission in the visible region are indicated.

[1] A. Bril and H. A. Klasens, Philips Res. Rept. **7**, 421 (1952).
[2] J. W. Gilliland and M. S. Hall, Electrochem. Tech. **4**, 378 (1966).
[3] E. Loh, Phys. Rev. **154**, 270 (1967).
[4] G. Blasse and A. Bril, Appl. Phys. Letters **11**, 53 (1967).

II. EXPERIMENTAL

Samples were prepared by firing intimate mixtures of high-purity oxides (or compounds, which on decomposition yield oxides) at appropriate temperatures in nitrogen. The Ce^{3+} ions were introduced by replacing part of the trivalent lanthanide ions by Ce^{3+} ions. The Ce^{3+} concentration was 1–2 at. %. Products were checked by x-ray analysis. The performance of the optical measurements has been described previously.[4–6]

III. REFLECTION AND EXCITATION SPECTRA

A. Results

Tables I–III contain the absorption bands of the Ce^{3+} ion in a number of host lattices in the uv region. These host lattices do not absorb in the optical region studied except for the Ga-containing oxides. The data were obtained from excitation and diffuse reflection spectra. In some cases only a continuous absorption was found, so that the absorption bands remain unknown (Table II). Figures 1–3 show the excitation and diffuse reflection spectra of $YAl_3B_4O_{12}$:Ce, $Y_3Al_5O_{12}$:Ce, and $ScBO_3$:Ce. These figures illustrate two types of excitation spectra, viz., those in which the quantum efficiency of the Ce^{3+} fluorescence is roughly independent of the exciting wavelength ($YAl_3B_4O_{12}$:Ce, Fig. 1) and those in which the quantum efficiency decreases

[5] A. Bril and W. L. Wanmaker, J. Electrochem. Soc. **111**, 1363 (1964).
[6] G. Blasse and A. Bril, J. Chem. Phys. **46**, 2579 (1967).

TABLE I. Efficiencies for ultraviolet and cathode ray excitation, positions of emission and excitation bands and Stokes shift of the emission of some Ce^{3+} phosphors.

Composition[a]	η(%)[b]	q_{max}(%)[c]	Emission bands (10^3 cm^{-1})[d]	Excitation bands (10^3 cm^{-1})[e]	Stokes shift (10^3 cm^{-1})[f]
$Sc_2Si_2O_7$–Ce	1.5	65	25.4; 29.4	29.0; 33.3; ~43.5	3.6
$ScBO_3$–Ce	2	70	26.8; ~30.5	28.0; 31.2; 36.1; 38.5	1.2
YBO_3–Ce	2	50	23.8; 25.4	27.4; (~29); 40.8; (~43.5)	2.0
$LaBO_3$–Ce	0.2	35	26.6; 28.4; 31.5	30.8; 36.9; 41.5	2.4
YPO_4–Ce	2.5	30	28.3; 30.0	32.8; (34.2); 39.6	2.8
$LaPO_4$–Ce	2.2	40	29.8; 31.5	36.2; 38.8; 41.6	4.7
$YAl_3B_4O_{12}$–Ce	2	40	27.2; 29.1	31.0; 36.6; 39.2	1.9
$Y_3Al_5O_{12}$–Ce	3.5	~70	18.2; 27.8; ~29.2	22.0; 29.4; ~37; ~44	3.8
YOCl–Ce	3.5	60	26.3	31.6; 35.8	5.3
LaOCl–Ce	0.4	30	27.8	(~35); 35.8; 39.7	5.2
LaOBr–Ce	0.2	25	22.8	28.4; 34.7	5.6

[a] Ce^{3+} concentration is 1–2 at.%.
[b] Radiant efficiency for cathode ray excitation (20 kV).
[c] Quantum efficiency for excitation in the lowest excited level.
[d] Position of the emission peaks.
[e] Position of the excitation bands; shoulders between brackets.
[f] Stokes shift of the emission, i.e., difference between the positions of the lowest excited level and the short-wavelength component of the emission from this level.

drastically with decreasing exciting wavelength ($Y_3Al_5O_{12}$–Ce, Fig. 2 and $ScBO_3$–Ce, Fig. 3). All the excitation spectra we obtained belong to either the former or the latter type. In this section we discuss the number and position of the absorption bands and a possible explanation for the two types of excitation spectra. A comparison between the excitation spectra of Ce^{3+}- and Tb^{3+}-activated phosphors is also included.

B. Discussion

The occurrence of more than one Ce^{3+} absorption band in the region between 25 000 and 50 000 cm^{-1} is due to the crystal-field splitting of the $5d$ (^2D) state. As argued before in the case of Tb^{3+} we can neglect the effect of spin–orbit splitting, since the spin–orbit parameter ζ_{5d} is about 10^3 cm^{-1}, whereas the crystal-field splitting amounts to 10^4 cm^{-1} or more.[7] For nearly all compounds mentioned in the tables the symmetry of the lanthanide site is known, so that it is possible to compare the experimentally observed number of $5d$ levels and the number expected from the site symmetry. Not in all cases a reasonable agreement was found. Consider, for example, YOCl–Ce and YPO_4–Ce. The respective site symmetries are C_{4v} and D_{2d}, so that 3 and 4 levels are expected. The experimental numbers (Table I) are 2 and 3, respectively. It cannot be excluded, however, that there are levels beyond the spectral limit of our apparatus (~220 mμ) or that lower symmetrical splittings remain hidden in the broad bands observed experimentally. We never observed more bands than expected from the site-symmetry. In Table IV we have tabulated those host lattices for which the number of levels observed experimentally agrees reasonably well with the number expected from site symmetry.

From these data the cubic crystal-field splitting Δ and the center of gravity of the $5d$ levels can be found, at least approximately. In $Y_3Al_5O_{12}$–Ce the Ce^{3+} ion occupies a distorted cube, so that the $5d$ level is split into a lower doublet and a higher triplet by the cubic component of the crystal field. Noncubic components cause a further splitting. Unfortunately we observed only two components of the triplet, which causes some uncertainty in the value of Δ and the position of the center of gravity. In $ScBO_3$–Ce and $Sc_2Si_2O_7$–Ce the

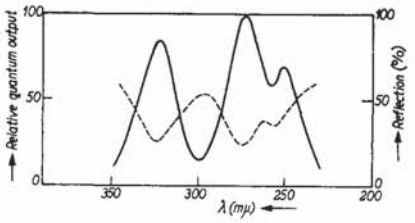

FIG. 1. Diffuse reflection spectrum (broken line) and relative excitation spectrum (solid line) of the Ce^{3+} fluorescence of $Y_{0.99}Ce_{0.01}Al_3B_4O_{12}$.

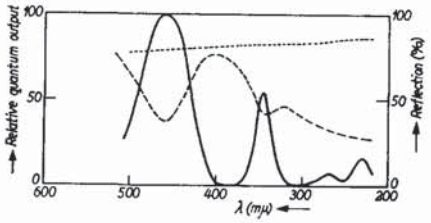

FIG. 2. Diffuse reflection spectrum (broken line) and relative excitation spectrum (solid line) of the Ce^{3+} fluorescence of $Y_{2.94}Ce_{0.06}Al_5O_{12}$. The dotted line represents the diffuse reflection spectrum of unactivated $Y_3Al_5O_{12}$.

[7] G. Blasse and A. Bril, Philips Res. Repts. **22**, 481 (1967).

TABLE II. Position of emission and excitation bands and Stokes shift of the emission of some Ce^{3+} phosphors (inefficient at room temperature).[a]

Composition	Emission bands (10^3 cm^{-1})	Excitation bands (10^3 cm^{-1})	Stokes shift (10^3 cm^{-1})
$Y_4Al_2O_9$–Ce	(~28); 31.2	32.6; ~34; ~41.5	~4.5
SrY_2O_4–Ce	17.4[b]	25.2; ?	~8
Y_2O_3–Ce	19.6; (~24)	?	...
$NaYO_2$–Ce	(~21.3); 22.8	?	...
$NaGdO_2$–Ce	21.3	?	...
$LaAlO_3$–Ce	...	24.2; 31.2; ~40[c]	...

[a] For explanation of columns see Table I. [b] At 77°K. [c] Data from reflection spectrum.

Ce^{3+} ion occupies distorted octahedra, so that the triplet is lower. In $YAl_3B_4O_{12}$–Ce the Ce^{3+} ion is in a trigonal prism of O^{2-} ions. The ^2D level splits into three levels with symmetry species E', A_1', and E'' (31 000, 36 600, and 39 200 cm^{-1}, respectively). This corresponds to a cubic crystal-field splitting of 6500 cm^{-1} (see Appendix).

Finally Table IV contains analogous data for SrF_2:Ce^{3+} recently given by Loh.[3] Although our results are not accurate, Table IV gives some interesting results. The $4f$–$5d$ distance is 51 000 cm^{-1} in the free Ce^{3+} ion. This value decreases to 48 000 cm^{-1} in fluorides and to roughly 35 000 cm^{-1} in oxides, a reduction of 6% and 30%, respectively. This fact must be ascribed to the reduction of the interelectronic repulsion parameters by covalency effects (nephelauxetic effect[8]). Within the group of oxidic host lattices there is even a variation of this value. For example, $ScBO_3$–Ce has the center of the $5d$ level at ~32 500 cm^{-1}. On the other hand, the value in the case of $LaPO_4$–Ce must be considerably higher than the 35 000 cm^{-1} mentioned above (see Table I). In our paper on Tb^{3+}-activated phosphors[7] we have already drawn attention to this fact. The Tb^{3+}-activated phosphors show excitation bands due to $4f \rightarrow 5d$ transitions in the Tb^{3+} ion. These bands are at higher wavenumbers than those of Ce^{3+} and partly beyond the shorter-wavelength limit of our apparatus, so that it was not possible to find the center of gravity in the case of Tb^{3+}.

Table IV also shows that the cubic crystal-field splitting Δ varies strongly. For a cube the absolute value of Δ is expected to be 8/9 times the value of Δ for an octahedron with the same distances between central ion and ligand.[9] With this in mind all values of Δ in Table IV can be compared with each other. The Δ in $Y_3Al_5O_{12}$–Ce is relatively large, whereas Δ in $YAl_3B_4O_{12}$–Ce is relatively small. That Δ is strongly influenced by the nature of the next-nearest neighbors is a well-known phenomenon.[10,11] We further note that Δ in the fluorides has the same order of magnitude as in the oxides. This has also been found for the transition-metal ions.[8]

The value of the noncubic crystal-field splitting varies considerably. For some host lattices it is possible to compare the splitting of the lower cubic crystal-field level of the $5d$ state of Ce^{3+} and the $4f^75d$ state of Tb^{3+}. The agreement is very good (Table V).

The phenomenon that the efficiency of Ce^{3+}-activated phosphors is more or less independent of the position of the excitation band in some cases (Fig. 1), but decreases strongly for excitation in bands with higher

TABLE III. Efficiency for cathode-ray excitation and position of the two lower absorption bands and of the emission band in the visible region for some Ce^{3+}-activated garnets.

Composition	η (%)	Position lower absorption bands (difference between brackets) (10^3 cm^{-1})	Emission bands in the visible region (10^3 cm^{-1})[a]
$Y_{1.5}Gd_{1.5}Al_5O_{12}$–Ce	...[b]	21.5, 29.6(8.1)	17.4
$Y_3Al_5O_{12}$–Ce	3.5	22.0, 29.4(7.4)	18.2
$Y_3Al_4GaO_{12}$–Ce	1.9	22.5, 29.1(6.6)	18.5
$Y_3Al_3Ga_2O_{12}$–Ce	1.7	23.0, 28.8(5.8)	19.2
$Y_3Al_2Ga_3O_{12}$–Ce	1.2	23.3, 28.6(5.3)	19.6(18.3)
$Y_3Ga_5O_{12}$–Ce	...	23.8, 28.1(4.3)	...[c]

[a] Shoulders between parentheses.
[b] Emission contains Eu^{3+} contributions due to the starting material Gd_2O_3, which contains a slight amount of europium.
[c] No fluorescence.

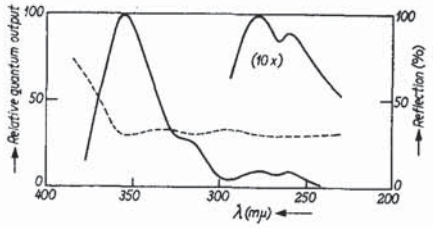

FIG. 3. Diffuse reflection spectrum (broken line) and relative excitation spectrum (solid line) of the Ce^{3+} fluorescence of $Sc_{0.99}Ce_{0.01}BO_3$.

[8] C. K. Jørgensen, *Absorption Spectra and Chemical Bonding* (Pergamon Press, Inc., New York, 1962).

[9] J. S. Griffith, *The Theory of Transition-Metal Ions* (Cambridge University Press, Cambridge, 1961).

[10] J. Ferguson, K. Knox, and D. C. Wood, J. Chem. Phys. **35**, 2236 (1961); **37**, 193 (1962).

[11] G. Blasse, J. Inorg. Nucl. Chem. **29**, 1817 (1967).

TABLE IV. The 5*d* levels and cubic crystal-field splitting (Δ) for Ce^{3+} in several host lattices. All values in 10^3 cm^{-1}.

Composition	Coordination of Ce^{3+}	5*d* levels (observed)[a]	Deduced cubic levels	Cubic crystal-field splitting (Δ)	Spherical 5*d*
$Y_3Al_5O_{12}$–Ce	Distorted cube (D_2)	22.0 29.4 | 37 44	25.7 (e_g), ~40 (t_{2g})	~14	~34.5
$YAl_3B_4O_{12}$–Ce	Trigonal prism (D_{3h})	31.0 36.6 39.2	...	~6.5[c]	35.4
$ScBO_3$–Ce	Distorted octahedron (D_{3d})	28.0 31.2 | 36.1 38.5	~29.5(t_{2g}), 37.3(e_g)	~8	~32.5
$Sc_2Si_2O_7$–Ce	Distorted octahedron (C_2)	29.0 33.3 | 43.5	~31(t_{2g}), ~43.5(e_g)	~12.5	~35
SrF_2–Ce[b]	Distorted cube	33.6 48.8 | 50.3 53.4	41.2(e_g), 52.4(t_{2g})	11.2	48
Free ion[b]	...	...	...	...	51

[a] Vertical bar indicates separation between lower and higher cubic levels.
[b] After Ref. 3.
[c] Value of the octahedral crystal-field splitting derived from the position of the levels for Ce^{3+} in prismatic coordination using a point-charge model (see Appendix).

wavenumbers in other cases (Figs. 2 and 3), is probably due to the position of the configuration coordinate curves relative to each other. Let us call the configuration coordinate curves of the ground state and the two lowest excited states g, e_1, and e_2, respectively (e_1 is below e_2). If the curve e_1 crosses the curve e_2 within the configuration coordinate curve of g, excitation into e_1 and e_2 may both result in efficient fluorescence from e_1. If on extrapolation the curves e_1 and e_2 should cross outside the curve g, however, excitation into e_1 gives efficient fluorescence from e_1, but excitation into e_2 cannot give efficient fluorescence from e_1, since either fluorescence from e_2 or radiationless transition to g results. If the "crossings" of e_2 with e_1 and g approach each other, weak fluorescence from e_1 and e_2 may be expected upon excitation into e_2. From this simple model it follows that a Ce^{3+}-activated phosphor with an excitation spectrum in which the efficiency decreases with increasing excitation energy, must show fluorescence from e_2 upon excitation into e_2 (or higher levels). This was in fact observed (see below).

IV. EMISSION

A. Results

The positions of the emission peaks of our samples are collected in Tables I–III. Figures 4-11 show the spectral energy distribution of the emission of a number of compounds. Usually the emission is in the near-uv region, but not always: $Y_3(Al, Ga)_5O_{12}$–Ce and SrY_2O_4–Ce (Figs. 5 and 10) show emission in the visible. The half-width value of the emission bands does not depend on their position and amounts to roughly 4000 cm^{-1} for all materials. In some cases the emission band is split, the difference between the two peaks being some 2000 cm^{-1} ($LaBO_3$–Ce, Fig. 4; YBO_3–Ce, Fig. 9; $YAl_3B_4O_{12}$–Ce and YPO_4–Ce, Table I). In many cases more than one emission band is present ($LaBO_3$–Ce, Fig. 4; $Y_3Al_5O_{12}$–Ce, Fig. 5; $ScBO_3$–Ce, Fig. 6; $Sc_2Si_2O_7$–Ce, Fig. 7; and $Y_4Al_2O_9$–Ce, Fig. 11).

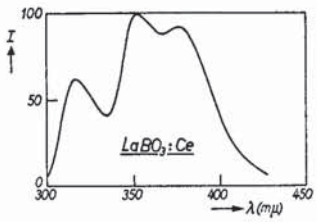

FIG. 4. Spectral energy distribution of the fluorescence of $La_{0.99}Ce_{0.01}BO_3$ under 254-mμ excitation. In Figs. 5–12 the radiant power per constant wavelength interval in arbitrary units (I) is plotted along the ordinate.

B. Discussion

The fluorescence emission of the Ce^{3+} ion originates from a transition from one or more of the 5*d* levels (often only the lowest level) to the ^2F ground state. Since the ground state of the Ce^{3+} ion is a doublet ($^2F_{5/2}$ and $^2F_{7/2}$) with a separation of about 2000 cm^{-1}, each emission band is expected to show two peaks as found by us in many cases (compare also Ref. 12). This doublet character of the emission band depends on temperature and Ce^{3+} concentration (self-absorption) and is not always found.[13]

In the case of oxidic host lattices this emission usually peaks in the near uv. As a matter of fact there are two

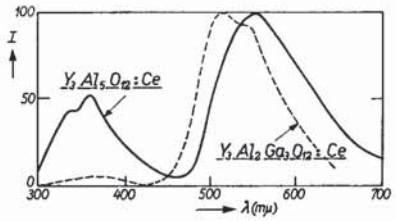

FIG. 5. Spectral energy distribution of the fluorescence of $Y_{2.94}Ce_{0.06}Al_5O_{12}$ (solid line) and $Y_{2.94}Ce_{0.06}Al_2Ga_3O_{12}$ (broken line) under 254-mμ excitation.

[12] F. A. Kröger and J. Bakker, Physica **8**, 628 (1941).
[13] Th. P. J. Botden, Philips Res. Rept. **7**, 197 (1952).

TABLE V. Splitting of the lower cubic crystal-field component of the $5d$ level of Ce^{3+} and the $4f^7 5d$ level of Tb^{3+} (all values in 10^3 cm^{-1}).

Host lattice	Ce^{3+} [a]	Tb^{3+} [b]
$Y_3Al_5O_{12}$	7.4	7.5
$Y_3Ga_5O_{12}$	4.3	4.0
YBO_3	~1.6	1.4
$Sc_2Si_2O_7$	4.3	4.6

[a] From Tables I and III.
[b] From Ref. 7.

cases in which the emission will be at lower wave numbers.

(a) If the lowest $5d$ level lies exceptionally low.
(b) If the Stokes shift of the emission is exceptionally large.

We have found one example of each of these two cases.

In $Y_3Al_5O_{12}$–Ce the lowest $5d$ level is exceptionally low, viz., at 22 000 cm^{-1} (see Table I). The $Y_3Al_5O_{12}$–Ce is the only Ce^{3+}-activated phosphor that has not a white, but a yellow body color, whereas the host lattice itself is white. Therefore, the emission lies also at very low wavenumbers. Note in Table I that the Stokes shift of this emission does not have a value deviating from what is normally found. Table IV shows, why the lowest $5d$ level lies so very low. The center of the $5d$ levels of Ce^{3+} in $Y_3Al_5O_{12}$ has a normal value. In Sec. III we have found that the crystal-field splitting in $Y_3Al_5O_{12}$ is very large. Moreover, the lower cubic level is the e_g level, which is $\frac{3}{5}\Delta$ below the center. In an octahedron the t_{2g} level is lower (only $\frac{2}{5}\Delta$ below the center). This means that the lower cubic crystal-field component is relatively low in $Y_3Al_5O_{12}$ (25 700 cm^{-1}, compared with ~30 000 cm^{-1} for the lower t_{2g} level of $ScBO_3$–Ce and $Sc_2Si_2O_7$–Ce). There is yet another effect, viz., the large noncubic splitting of the e_g level of Ce^{3+} in $Y_3Al_5O_{12}$, which brings the lowest level at 22 000 cm^{-1}. Visible Ce^{3+} emission can therefore be expected, if the $5d$ crystal-field splitting and the lower symmetrical splitting are large. Cubic eight coordination is also favorable to obtain visible emission, because the lower cubic level will then be at relatively low energies.

It is obvious that long-wavelength emission will also result in the case of a very large Stokes shift. This is the case for SrY_2O_4–Ce. The lowest $5d$ level is not exceptionally low (25 200 cm^{-1}), but the Stokes shift is very large (~8000 cm^{-1}, compare Tables I and II), so that visible emission results (Fig. 10), Such a large Stokes shift can only occur if the difference between the equilibrium distance of the excited state and that of the ground state is larger than usual. Elsewhere[14] we have argued that the increase of the equilibrium distance upon excitation will be large if the ions of the host lattice are rather weakly bounded together, i.e., if large and low-charged ions are involved (this implies ions with relatively highly polarization or, as they are sometimes called, "soft" ions[15]). Such a situation exists in SrY_2O_4. We also noted weak fluorescence in the visible region in the case of Y_2O_3–Ce, $NaYO_2$–Ce, and $NaGdO_2$–Ce (Table II). These are also lattices with large cations. The same holds for YOCl–Ce, LaOCl–Ce, and LaOBr–Ce (Table I), but the oxychlorides emit in the uv. Note, however, that the Stokes shift of these materials is also large.

Another consequence of a large increase of the equilibrium distance upon excitation is a low quenching temperature of the fluorescence. For SrY_2O_4–Ce we found that the light output at 200°K is only 20% of the output at 100°K. Such a marked temperature dependence agrees with out model. In a number of other lattices with large ions (Sr_2LaAlO_5–Ce, $SrLaAlO_4$–Ce, $LaAlO_3$–Ce) the Ce^{3+} emission was absent or only very weak, even at liquid-nitrogen temperature.

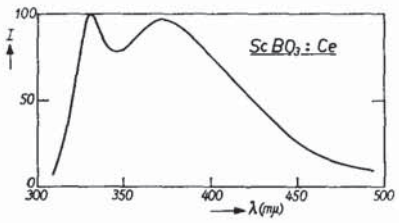

FIG. 6. Spectral energy distribution of the fluorescence of $Sc_{0.99}Ce_{0.01}BO_3$ under 254-mμ excitation.

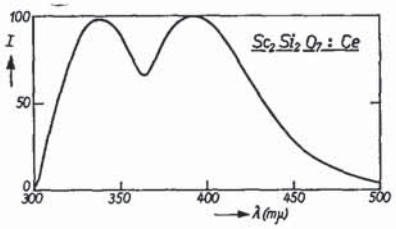

FIG. 7. Spectral energy distribution of the fluorescence of $Sc_{1.98}Ce_{0.02}Si_2O_7$ under 254-mμ excitation.

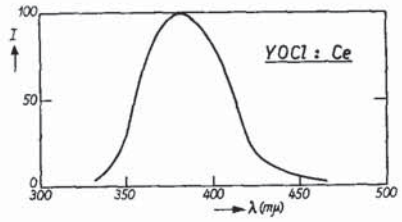

FIG. 8. Spectral energy distribution of the fluorescence of $Y_{0.99}Ce_{0.01}OCl$ under 254-mμ excitation.

[14] G. Blasse and A. Bril, Z. Physik. Chem. (Frankfurt) "The influence of crystal structure on the fluorescence of oxidic niobates and related compounds" (to be published).
[15] Compare C. K. Jørgensen, Coord. Chem. Rev. 1, 164 (1966).

DOCKET ALARM

Explore Litigation Insights

Docket Alarm provides insights to develop a more informed litigation strategy and the peace of mind of knowing you're on top of things.

Real-Time Litigation Alerts

Keep your litigation team up-to-date with **real-time alerts** and advanced team management tools built for the enterprise, all while greatly reducing PACER spend.

Our comprehensive service means we can handle Federal, State, and Administrative courts across the country.

Advanced Docket Research

With over 230 million records, Docket Alarm's cloud-native docket research platform finds what other services can't. Coverage includes Federal, State, plus PTAB, TTAB, ITC and NLRB decisions, all in one place.

Identify arguments that have been successful in the past with full text, pinpoint searching. Link to case law cited within any court document via Fastcase.

Analytics At Your Fingertips

Learn what happened the last time a particular judge, opposing counsel or company faced cases similar to yours.

Advanced out-of-the-box PTAB and TTAB analytics are always at your fingertips.

API

Docket Alarm offers a powerful API (application programming interface) to developers that want to integrate case filings into their apps.

LAW FIRMS
Build custom dashboards for your attorneys and clients with live data direct from the court.

Automate many repetitive legal tasks like conflict checks, document management, and marketing.

FINANCIAL INSTITUTIONS
Litigation and bankruptcy checks for companies and debtors.

E-DISCOVERY AND LEGAL VENDORS
Sync your system to PACER to automate legal marketing.